ChemComm

This article is part of the

New advances in catalytic C–C bond formation via late transition metals web themed issue

Guest editor: Professor Michael Krische

All articles in this issue will be gathered together online at www.rsc.org/catalytic_CC.

ChemComm

Dynamic Article Links

Cite this: *Chem. Commun.*, 2012, **48**, 263–265

www.rsc.org/chemcomm

COMMUNICATION

Two-stage optimization of a supramolecular catalyst for catalytic asymmetric hydroboration†‡

Shin A. Moteki,§[a] Kazuya Toyama,[a] Zeyu Liu,[b] Jing Ma,[b] Andrea E. Holmes[c] and James M. Takacs*[a]

Received 3rd October 2011, Accepted 2nd November 2011
DOI: 10.1039/c1cc16146f

Systematic changes, first to the structure of the catalyst scaffold and then to the ligating groups, are used to fine tune supramolecular catalysts to achieve high regioselectivity (95–98%) and high enantioselectivity (94–97% ee) across a series of *meta*-substituted styrenes varying in electronic character.

Combining bisoxazoline subunits **1** of complementary chirality with Zn(II) affords the thermodynamically favored heteroleptic zinc complex **2**. By virtue of the modular design, a series of bifunctional subunits bearing a chiral monophosphite connected to the bisoxazoline moiety *via* a phenyl or biphenyl tether can be used to create dozens of distinct self-assembled ligands (SALs) **2**, each possessing a slightly different ligand scaffold. When combined with metal catalysts, these SALs afford closely related, but structurally unique, heterobimetallic supramolecular catalysts differing subtly in the catalyst scaffold.[1]

While great strides have been made toward mimicking catalytic behaviours of enzymes using supramolecular coordination catalysts,[2] other than efficient screening methods,[3] the protocol for optimizing the performance of a supramolecular catalyst is not as well developed as those for traditional homogeneous catalysts.[4] The present study focuses on using a two-step optimization strategy, first ligand/catalyst scaffold and then ligating group optimization, to identify catalysts that rival or exceed the best selectivity previously reported for the catalytic asymmetric hydroboration (CAHB)[5] of a series of *meta*-substituted styrenes.[6] Methods for catalytic asymmetric synthesis of chiral organoboranes and related derivatives are of renewed interest,[7–9] principally due to the recent development of stereospecific methods for their use in C–C bond construction.[10]

A series of 64 SALs **Zn(^{S}Xa,^{R}Ya) (2)**, each bearing the parent TADDOL-derived phosphite **a**, were prepared *in situ via* combination of the appropriate subunits **^{S}Xa** and **^{R}Ya**. These were evaluated under a standard set of reaction conditions for the rhodium-catalyzed CAHB of 3-methylstyrene (**3a**, X = Me) by pinacolborane (PinBH). Enantioselectivity is determined by chiral GC analysis after oxidative workup. The catalysts screened exhibit enantioselectivities that vary over a wide range, distributing rather smoothly from near racemic to greater than 90% ee (Fig. 1). The catalyst derived from SAL **Zn(^{S}Aa,^{R}Aa)** is among the better ones, effecting CAHB of **3a** to (*S*)-**4a** in 91% ee and with excellent regiocontrol (98%) (Table 1, entry 1).[11]

The data in entries 2–4 of Table 1 highlight the results of some key control experiments. Adding the complementary **^{S}Aa** and **^{R}Aa** subunits but omitting zinc (entry 2) gives lower yield, enantioselectivity and regioselectivity than SAL **Zn(^{S}Aa,^{R}Aa)**. Using two equivalents of a truncated SAL containing the zinc complex but lacking one of the two phosphite moieties (*i.e.*, **Zn(^{S}Aa,^{R}D)**, entry 3) gives similar results. The results obtained in these latter two cases are very similar to those obtained using two equivalents of the chiral monophosphite (TADDOL)POPh (entry 4). These experiments show the positive effect of the

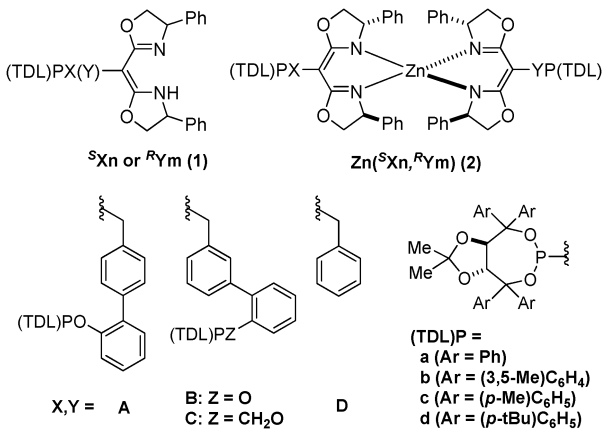

Fig. 1 A subset of chiral bisphosphite SALs, **Zn(^{S}Xn,^{R}Ym) (2)**, prepared *via* chirality directed self-assembly of subunits **^{S}Xn** and **^{R}Ym** using combinations of tethers (*e.g.*, **X** and **Y** = **A–B**) bearing chiral phosphite ligating groups (TDL)P from among **a–d**.

[a] *Department of Chemistry, University of Nebraska-Lincoln, Lincoln, Nebraska, USA. E-mail: jtakacs1@unl.edu; Fax: +1 402 472 9402; Tel: +1 402 472 6232*
[b] *School of Chemistry and Chemical Engineering, Institute of Theoretical and Computational Chemistry, Key Laboratory of Mesoscopic Chemistry of MOE, Nanjing University, Nanjing, Jiangsu 210093, People's Republic of China*
[c] *Department of Chemistry, Doane College, Crete, Nebraska 68333, USA*

† This article is part of the *ChemComm* 'Advances in catalytic C–C bond formation via late transition metals' web themed issue.

‡ Electronic supplementary information (ESI) available: Detailed procedures and compound characterization. See DOI: 10.1039/c1cc16146f

§ Present address: Laboratory for Specially-Promoted Research on Organocatalytic Chemistry, Kyoto University, Kyoto, Japan.

Table 1 Rhodium-catalyzed CAHB of **3a** using SAL **Zn(**^{S}**Aa,**^{R}**Aa)**[a]

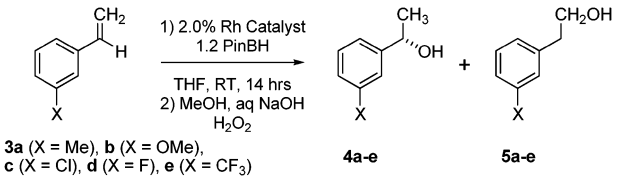

3a (X = Me), **b** (X = OMe), **c** (X = Cl), **d** (X = F), **e** (X = CF_3) — **4a-e** — **5a-e**

Entry	RhX	Ligand	% ee of **4a** (% α-isomer **4a**)
1	BF_4	**Zn(**^{S}**Aa,**^{R}**Aa)**	91 (98)
2[b]	BF_4	^{S}**Aa** + ^{R}**Aa**	73 (90)
3[c]	BF_4	**Zn(**^{S}**Aa,**^{R}**D)**	73 (85)
4[c]	BF_4	(TADDOL)POPh	70 (81)

[a] Reaction conditions: 2% $Rh(nbd)_2BF_4$, 2% SAL, 1.2 equiv. of Pin BH, THF, rt, 14 h; yields are essentially quantitative. [b] Only subunits ^{S}**Aa** and ^{R}**Aa**, no zinc present. [c] Two equivalents of monophosphite.

ligand scaffold on catalyst performance and suggest that a chelated SAL–Rh complex is important to the success of entry 1.

Fig. 2 compiles the results obtained for the 64 catalysts with 3-methylstyrene (**3a**) and four other *meta*-substituted styrenes (*i.e.*, **3b–e**). Enantioselectivity is expressed in terms of $\Delta\Delta G^{\ddagger}$ for the competing pathways leading to (*R*)- and (*S*)-**4** and ordered from the most to the least enantioselective catalyst based on results obtained for **3a**. While the different catalyst scaffolds effect CAHB with different degrees of efficiency, it is noteworthy that the enantioselectivity exhibited by a given catalyst often varies little across the series of substrates; this is especially seen for the more selective catalysts, *e.g.*, **Zn(**^{S}**Aa,**^{R}**Aa)** (90–92% ee, Table 2, entry 1). The data indicate that the substituent does not strongly influence enantioselectivity in a systematic way.[12]

Catalyst scaffolds derived from tethers **A** and **B** exhibit high selectivity. These were used in a second stage of catalyst optimization focusing on varying the shape of the TADDOL ligating group by employing different aryl substituents.[13] Entries 1–4 in Table 2 use tether **A** with each of the TADDOL-phosphites **a–d**. The 3,5-dimethyl-derivative, TADDOL **b** (entry 2), did not significantly impact enantioselectivity but did lower regioselectivity (see ESI‡). The 4-methylphenyl derivative, TADDOL **c** (entry 3), exhibits the high regioselectivity seen for TADDOL **a** and improves

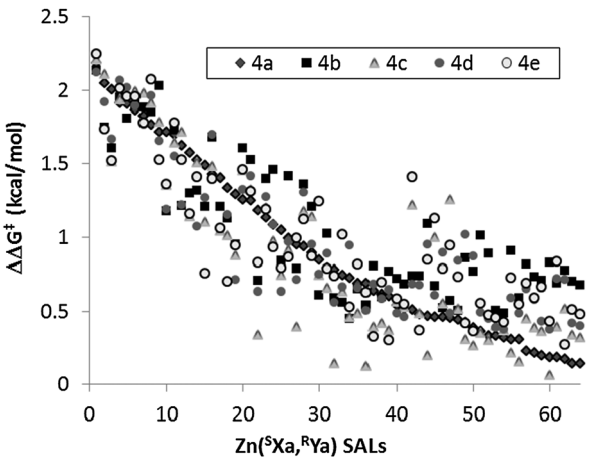

Fig. 2 Enantioselectivity (expressed in terms of $\Delta\Delta G^{\ddagger}$) for CAHB leading to (*R*)- and (*S*)-**4a–e** with 64 supramolecular catalysts.

Table 2 Subtle variation of the ligating group further optimizes the (SAL)Rh-catalyzed CAHB of **3a–e**[a]

	^{S}Xn	^{R}Xn	4a	4b	4c	4d	4e
1	**Aa**	**Aa**	91	90	91	92	90
2	**Ab**	**Ab**	91	90	90	91	91
3	**Ac**	**Ac**	84	92	96	95	95
4	**Ad**	**Ad**	57	70	75	78	83
5[b]	**Ab**	**Ac**	94	95	94	94	94
6[c]	**Ab**	**Ac**	94	93	94	93	93
7	**Ac**	**Bc**	88	95	92	92	97
8	**Bc**	**Ac**	90	95	92	90	95
9	**Bc**	**Bc**	92	93	94	96	95
10	**Bc**	**Cc**	88	90	90	90	90

[a] Screening conditions: 2% $Rh(nbd)_2BF_4$, 2.1% SAL, 1.2 PinBH, THF, rt, 14 h. Data reported as % ee of **4**. [b] 0.8 mol% catalyst. [c] 1.0 mmol substrate, 0.05% $Rh(nbd)_2BF_4$, 0.05% SAL, 1.2 PinBH, THF, rt, 5 h.

the enantioselectivity for 4 of the 5 substrates. The *tert*-butyl derivative (TADDOL **d**, entry 4) gives only moderate enantioselectivity. Incorporating two different ligating groups into the SAL can further tune catalyst performance. For example, the catalyst derived from the heterocombination SAL **Zn(**^{S}**Ab,**^{R}**Ac)** (entry 5) shows better performance than either **Zn(**^{S}**Ab,**^{R}**Ab)** or **Zn(**^{S}**Ac,**^{R}**Ac)** and is effective at rather low catalyst loading (0.05 mol%, entry 6).

Combining different tethers can be effective. Diastereomeric SALs **Zn(**^{S}**Ac,**^{R}**Bc)** and **Zn(**^{S}**Bc,**^{R}**Ac)** are particularly effective for the methoxy-(**3b**) and trifluoromethyl-derivatives (**3e**). The highest enantioselectivity for the fluoro-derivative (**3d**) is obtained with the catalyst derived from **Zn(**^{S}**Bc,**^{R}**Bc)**. Overall, systematic changes in the structure of the TADDOL ligating group permit fine tuning of the supramolecular catalyst to achieve high enantioselectivity (94–97% ee) and high regioselectivity (95–98%; see ESI‡, Table S2 for details) across the series **3a–e**.

As for the nature of the catalyst, several lines of evidence in addition to those experiments discussed above in the context of Table 1 suggest that 1 : 1 SAL : Rh chelated structures are relevant. For example, there are major changes in the circular dichroic (CD) spectra upon complexation to rhodium (Fig. 3). The CD spectrum of SAL **Zn(**^{S}**Bc,**^{R}**Ac)** in dichloromethane exhibits a bisignate couplet with a zero-crossing at around 316 nm. The bisignate couplet indicates exciton coupling with negative chirality.[14] In contrast, its rhodium complex (*i.e.*, [**Zn(**^{S}**Bc,**^{R}**Ac)**Rh(nbd)]BF_4) shows a new negative Cotton effect in the region around 243 nm[15] but no bisignate CD is apparent. In rigid systems, this type of negative bisignate CD is associated with a negative absolute twist between the electric transition moments of interacting chromophores.[16] The disappearance of this signal indicates a loss of a helical arrangement in conjunction with a conformational change

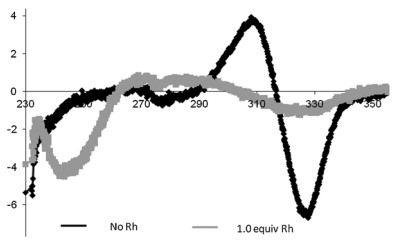

Fig. 3 CD spectra (230–350 nm in CH_2Cl_2) of SAL **Zn(**^{S}**Bc,**^{R}**Ac)** (black trace) and [**Zn(**^{S}**Bc,**^{R}**Ac)**Rh(nbd)]BF4 (gray).

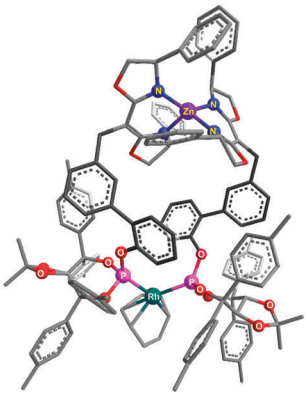

Fig. 4 Modeled structure of the *cis*-[**Zn(**^{S}**Bc,**^{R}**Bc)**Rh(cod)]$^{+}$ complex.

in going from the free SAL, **Zn(**^{S}**Bc,**^{R}**Ac)**, to the rhodium complex, [**Zn(**^{S}**Bc,**^{R}**Ac)**Rh(nbd)]BF_4.

The rhodium complex of **Zn(**^{S}**Bc,**^{R}**Cc)** (Table 2, entry 10), while not as efficient as the **Zn(**^{S}**Bc,**^{R}**Bc)** catalyst, is amenable to structural characterization. HRFAB mass spectrometry finds a peak at 2363.8108 *m*/*z*, consistent with the heterobimetallic complex, [**Zn(**^{S}**Bc,**^{R}**Cc)**Rh(nbd)]BF_4 (calculated 2363.8009 *m*/*z*). The ^{31}P NMR spectrum of the complex is simple and clean, exhibiting peaks at 107.7 and 113.6 ppm with Rh–P couplings of 249 and 254 Hz, respectively, and P–P coupling of 38.8 Hz.

DFT calculations at the B3LYP/6-31G (non-metal atoms) and B3LYP/LanL2DZ (metal atoms) levels were carried out to explore the possible conformations of *cis*-[**Zn(**^{S}**Bc,**^{R}**Bc)**Rh(cod)]$^{+}$. Fig. 4 presents the predicted most stable conformer from among several possible configurations (see ESI‡). Its structure gives some preliminary indications of ways in which the ligand/catalyst scaffold and ligating group substituents influence the topography around rhodium.

In summary, a series of SALs, each bearing the parent TADDOL-derived ligating group, was used in the CAHB of five *meta*-substituted styrenes varying in steric and electronic character. The results show that enantioselectivity as a function of catalyst scaffold varies similarly for all five substrates. This suggests that enantioselectivity is not strongly correlated with the nature of the substituent in this series. Scaffolds incorporating tethers **A** and **B** prove to be among the most efficient catalysts. These were further optimized by varying the aryl substituents on the TADDOL moiety. In some cases, the most efficient catalyst combines two different ligating groups in the SAL. Overall, systematic changes in the structures of the scaffold and ligating groups permit fine tuning of the supramolecular catalyst to achieve high regioselectivity (95–98%) and high enantioselectivity (94–97% ee) across the series of five substrates, **3a–e**. The results rival or exceed the best selectivity previously reported for each substrate. Computational modelling gives a picture of the presumed 1 : 1 chelated structure and provides a starting point for probing structure activity relationships in future studies.

Financial support for this research from the NSF (CHE-0809637) is gratefully acknowledged. We thank A. Vidol (ICREA) for preliminary studies modeling the CD spectra, N. C. Thacker for assistance in the preparation of this manuscript, the NSF (CHE-0091975, MRI-0079750) and NIH (SIG-1-510-RR-06307) for the NMR spectrometers used in these studies carried out in facilities renovated under NIH RR016544.

Notes and references

1 J. M. Takacs, P. M. Hrvatin, J. M. Atkins, D. S. Reddy and J. L. Clark, *New J. Chem.*, 2005, **29**, 263–265; J. M. Takacs, D. S. Reddy, S. A. Moteki, D. Wu and H. Palencia, *J. Am. Chem. Soc.*, 2004, **126**, 4494–4495; J. M. Takacs, K. Chaiseeda, S. A. Moteki, D. S. Reddy, D. Wu and K. Chandra, *Pure Appl. Chem.*, 2006, **78**, 501–509.

2 (*a*) M. J. Weister, P. A. Ulmann and C. A. Mirkin, *Angew. Chem., Int. Ed.*, 2011, **50**, 114–137; (*b*) S. Carboni, C. Gennari, L. Pignataro and U. Piarulli, *Dalton Trans.*, 2011, **40**, 4355–4373; (*c*) J. Meeuwissen and J. N. H. Reek, *Nat. Chem.*, 2010, **2**, 615–621; (*d*) G. Gasparini, M. D. Molin and L. J. Prins, *Eur. J. Org. Chem.*, 2010, 2429–2440; (*e*) P. W. N. M. van Leeuwen, Supramolecular Catalysis, Wiley-VCH, Weinhem, 2008; (*f*) S. J. Reyes and K. Burgess, *Chem. Soc. Rev.*, 2006, **35**, 416–423; (*g*) B. Breit, *Angew. Chem., Int. Ed.*, 2005, **44**, 6816–6825; (*h*) E. A. Karakhanov, A. L. Maksimiov and E. A. Runova, *Russ. Chem. Rev.*, 2005, **74**, 97–111.

3 J. Wieland and B. Breit, *Nat. Chem.*, 2010, **2**, 832–837.

4 J. M. Brown and R. J. Deeth, *Angew. Chem., Int. Ed.*, 2009, **48**, 4476–4479, and references cited therein.

5 Reviews: A. M. Carroll, T. P. O'Sullivan and P. J. Guiry, *Adv. Synth. Catal.*, 2005, **347**, 609–631; C. M. Vogels and S. A. Westcott, *Curr. Org. Chem.*, 2005, **9**, 687–699; C. M. Crudden and D. Edwards, *Eur. J. Org. Chem.*, 2003, 4695–4712; I. Beletskaya and A. Pelter, *Tetrahedron*, 1997, **53**, 4957–5026; K. Burgess and M. J. Ohlmeyer, *Chem. Rev.*, 1991, **91**, 1179–1191.

6 A previous study on the CAHB of *ortho*-substituted styrenes showed the effectiveness of ligand/catalyst scaffold optimization. See: S. A. Moteki and J. M. Takacs, *Angew. Chem., Int. Ed.*, 2008, **47**, 894–896. The two-step optimization protocol described herein has subsequently been used to further improve catalyst performance.

7 For recent examples of catalyzed hydroborations of 1,3-dienes, see: R. J. Ely and J. P. Morken, *J. Am. Chem. Soc.*, 2010, **132**, 2534–2535; Y. Sasaki, C. Zhong, M. Sawamura and H. Ito, *J. Am. Chem. Soc.*, 2010, **132**, 1226–1227; J. Y. Wu, B. Morequ and T. Ritter, *J. Am. Chem. Soc.*, 2009, **131**, 12915–12917.

8 For recent examples of enantioselective β-borations of α,β-unsaturated carbonyls, see: A. Guzman-Martinez and A. H. Hoveyda, *J. Am. Chem. Soc.*, 2010, **132**, 10634–10637; I. Chen, M. Kanai and M. Shibasaki, *Org. Lett.*, 2010, **12**, 4098–4101; D. Noh, H. Chea, J. Ju and J. Yun, *Angew. Chem., Int. Ed.*, 2009, **48**, 6062–6064.

9 For recent examples of enantioselective diboration, see: C. H. Schuster, B. Li and J. P. Morken, *Angew. Chem., Int. Ed.*, 2011, **50**, 7906–7909; L. T. Kliman, S. N. Mlynarski and J. P. Morken, *J. Am. Chem. Soc.*, 2009, **131**, 13210–13211; H. E. Burks and J. P. Morken, *Chem. Commun.*, 2007, 4717–4725 and references cited therein.

10 D. L. Sandrock, L. Jean-Gerard, C.-Y. Chen, S. D. Dreher and G. A. Molander, *J. Am. Chem. Soc.*, 2010, **132**, 17108–17110; T. Ohmura, T. Awano and M. Suginome, *J. Am. Chem. Soc.*, 2010, **132**, 13191–13192; A. Ros and V. K. Aggarwal, *Angew. Chem., Int. Ed.*, 2009, **48**, 6289–6292; D. Imao, B. W. Glasspoole, V. S. Laberge and C. M. Crudden, *J. Am. Chem. Soc.*, 2009, **131**, 5024–5025; C. M. Crudden, B. W. Glasspoole and C. J. Lata, *Chem. Commun.*, 2009, 6704–6716 and references cited therein.

11 For CAHB of **3a** in as high as 91% ee, see: S. Demay, F. Volant and P. Knochel, *Angew. Chem., Int. Ed.*, 2001, **40**, 1235–1238.

12 The efficiency, regioselectivity and enantioselectivity of vinyl arene CAHB are thought to depend upon both steric and electronic influences of aryl substituents, see: A. M. Segarra, E. Daura-Oller, C. Claver, J. M. Poblet, C. Bo and E. Fernandez, *Chem.–Eur. J.*, 2004, **10**, 6456–6467; D. R. Edwards, Y. B. Hleba, C. J. Lata, L. A. Calhoun and C. M. Crudden, *Angew. Chem., Int. Ed.*, 2007, **46**, 7799–7802; A. C. Maxwella, S. P. Flanagana, R. Goddard and P. J. Guiry, *Tetrahedron: Asymmetry*, 2010, **21**, 1458–1473 and references therein.

13 D. Seebach, A. K. Beck and A. Heckel, *Angew. Chem., Int. Ed.*, 2001, **40**, 92–138.

14 N. Harada and K. Nakanishi, *Circular Dichroic Spectroscopy. Exciton Coupling in Organic Stereochemistry*, University Science Books, Mill Valley, CA, 1983.

15 A similar peak is seen in the CD upon the addition of $Rh(nbd)_2BF_4$ to (TADDOL)POPh in 1 : 2 stoichiometry.

16 I. Akritopoulou-Zanze, K. Nakanishi, H. Stepowska, B. Grzeszczyk, A. Zamojski and N. Berova, *Chirality*, 1997, **9**, 699–712.